SAKARYA ÜNİVERSİTESİ
FEN BİLİMLERİ ENSTİTÜSÜ DERGİSİ

Sakarya University Journal of Science
SAUJS

ISSN 1301-4048 e-ISSN 2147-835X Period Bimonthly Founded 1997 Publisher Sakarya University
http://www.saujs.sakarya.edu.tr/

Title: A New Gradient-Based Surface Defect Detection Method for the Ceramic Tile

Authors: Murat Alparslan GÜNGÖR

Recieved: 2021-12-17 00:00:00

Accepted: 2022-10-10 00:00:00

Article Type: Research Article

Volume: 26
Issue: 6
Month: December
Year: 2022
Pages: 1159-1169

How to cite
Murat Alparslan GÜNGÖR; (2022), A New Gradient-Based Surface Defect Detection Method for the Ceramic Tile. Sakarya University Journal of Science, 26(6), 1159-1169, DOI: 10.16984/saufenbilder.1038022
Access link
https://dergipark.org.tr/en/pub/saufenbilder/issue/74051/1038022

Sakarya University Journal of Science 26(6), 1159-1169, 2022

A New Gradient-Based Surface Defect Detection Method for the Ceramic Tile

Murat Alparslan GÜNGÖR*[1]

Abstract

Ceramic tiles are controlled to detect surface defects after production because many defects may occur on their surface during production. The detection of ceramic tile surface defects is usually performed by human observations in most factories. In this paper, an image processing method was proposed to detect the defects. In the proposed method, first, the user selects the homogenous region in the image. Then the gradient-based image processing algorithm is applied. We conducted our study using simulated and real images to which we applied the conventional image processing methods and our proposed method. Performance of the proposed method was evaluated with quality metric and subjective evaluation. The obtained results demonstrate that the proposed method has very good performance and is very promising for ceramic tile application.

Keywords: Ceramic tile, surface defect, defect detection, image processing

1. INTRODUCTION

Nowadays, the ceramic tile (CT) industry is a very important sector, but in the production of CTs, many surface defects occur such as cracks, edges, holes, and pinholes [1, 2]. Human vision control can be used for the detection of defective products. This depends on human experience and expertise. Thus, using image processing in the CT industry becomes very important for an effective, objective, and repetitive evaluation. This is done by computers automatically without or with little human intervention [3].

The block diagram of the defect detection algorithm is shown in Fig. 1 [4]. The first stage in the pre-processing step is image acquisition. In this stage, the CT image is captured from the real-world source and stored into a computer for further processing. The captured image is in the RGB format and is converted to gray-scale format. Then various operations such as contrast stretching, noise reduction, and image cropping are performed to realize a more effective defect detection algorithm [3, 5, 6]. Finally, the defect detection methods are applied.

Up to now, various methods have been proposed to detect surface defects. One of the

* Corresponding author: alparslangungor@hitit.edu.tr
[1] Hitit University, Faculty of Engineering, Department of Electrical and Electronics Engineering
ORCID: https://orcid.org/0000-0001-7446-7808

methods is selecting an appropriate threshold. Ng [7] proposed a thresholding approach based on the Otsu method. The proposed method is effective, simple and fast for defect detection. Hocenski et al. [8] focused on detecting one kind of defect, and highly contrasted dot shaped formation of pixels. To find highly contrasted dot shaped formations, they proposed the convolution-based method with local intensity difference analysis. The presented method shows better performance than similar methods but is less accurate than any complex morphology analysis-based method. Shire et al. [6] compared reference and test images to decide the defect after pre-processing operations but the proposed method is useful only for plain ceramic tiles. Sioma [9] presented 3D image analysis to evaluate defects on the surface of ceramic tiles and successful results were obtained for quick defect detection in automated control systems installed on production lines. Latif-Amet et al. [10] used wavelet transform for texture defect detection. Considering computational complexity and reliability, their approach is feasible for real-time applications. In [4], the Rotation Invariant Measure of Local Variance operator was employed for surface defect detection. The proposed system has high accuracy and can be used for the detection and classification of ceramic tile defects that occured in firing unit. Sobel, Prewitt and Canny edge detectors are gradient-based edge detection methods used to find the edge pixel in an image. These detectors have been employed in many studies for the surface defect detection of ceramic tiles [3, 11-13].

In this paper, a new gradient-based surface defect detection method for ceramic tile was proposed. In the proposed method, one or more homogeneous regions in the image are selected first. According to the selected regions, a threshold value and mean pixel value are calculated. Then, the gradient-based algorithm is applied using these values. We present, in detail, the proposed method and the materials used to assess the performance of the proposed method in Section 2. The proposed method is evaluated in Section 3 and our conclusions are presented in Section 4.

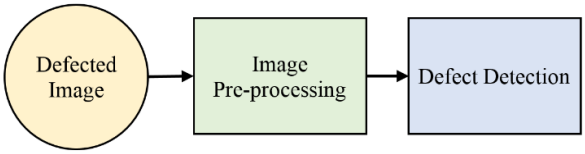

Figure 1 Block diagram of the defect detection algorithm

2. MATERIALS AND METHOD

The proposed method was applied to CT images having surface defects and compared with the existing gradient-based methods. The performance of the proposed method was evaluated with image quality metric and subjective evaluation.

2.1. Image Quality Metric and CT Images

In our study, we used real and simulated CT images. Performance was evaluated both objectively and subjectively. For objective evaluation, the first type of image used in this paper was the real CT images (these images were also used in [4]) shown in Fig. 2. The images in Fig. 2 are in the RGB format and they were converted to gray-scale format based on the NTSC conversion formula as Eq. (1), used in the image processing toolbox of MATLAB [14].

$$rgb2gray = 0.2989R + 0.587G + 0.114B \quad (1)$$

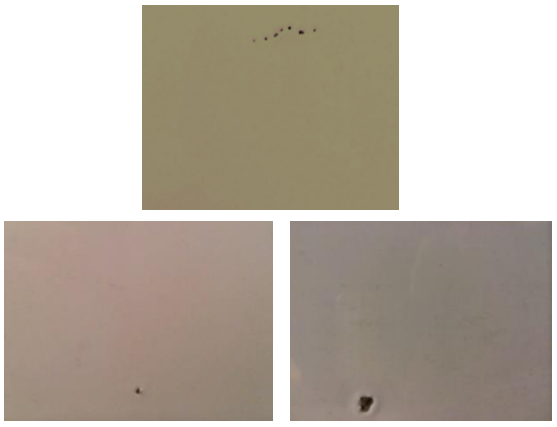

Figure 2 Real CT images for objective evaluation

The obtained gray level images are shown in Fig. 3. We named the images in Fig. 3a, Fig.3b and Fig. 3c as RI1, RI2 and RI3 (RI=Real Image), respectively. As shown in the images, all of them have one or more defective regions.

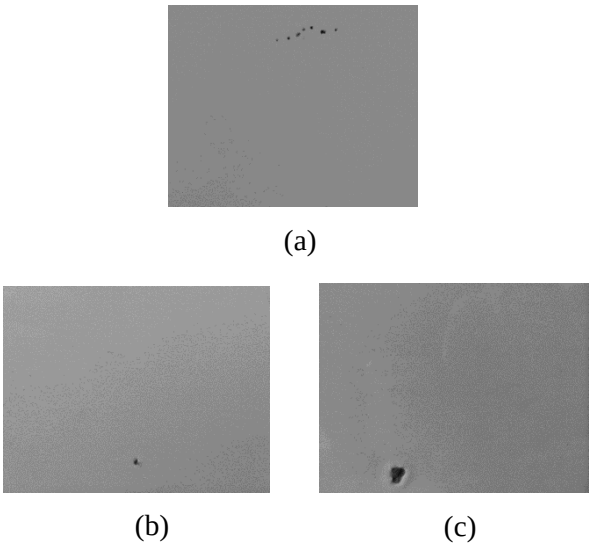

(a)

(b) (c)

Figure 3 The gray level CT images (a) RI1 (b) RI2 (c) RI3

The second type of image used in this paper was the simulated image shown in Fig. 4 for objective evaluation. We named the images in Fig. 4a, Fig.4b and Fig. 4c as SI1, SI2 and SI3 (SI=Simulated Image), respectively. The SIs were created using MATLAB [14]. The pixel values of the SIs are 210 except in the defective regions. The pixel values of the defective regions are zero in the SIs.

Any surface defect detection method aims to find pixels in the defective regions. The quality metric, the detection accuracy rate (%) (DAR) [4], is used for objective evaluation of the method, defined by:

$$DAR = \frac{A+D}{A+B+C+D} * 100 \quad (2)$$

where A is the number of the defective pixels, which are detected as defective pixels; D is the number of the non-defective pixels, which are detected as non-defective pixels; B is the number of the pixels detected as defect, but these are non-defective pixels; C is the number of the pixels detected as non-defect, but these are defective pixels. The DAR value is between 0 and 100. The higher this value, the better the performance of the applied method.

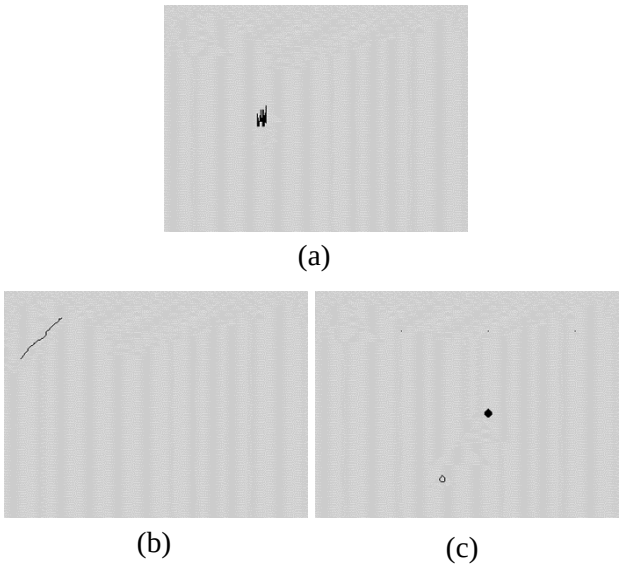

(a)

(b) (c)

Figure 4 The simulated images (a) SI1 (b) SI2 (c) SI3

2.2. Existing Gradient-Based Methods for Defect Detection

In this paper, we developed a new gradient-based surface defect detection method for ceramic tile. Sobel [15], Prewitt [16] and Canny [17] edge detectors which are gradient-based methods have been employed in many studies for defect detection. Canny implements a multi-step algorithm, while Sobel and Prewitt usually use 3*3 masks for the detection of edges. The purpose of these methods is to obtain the edges of the defective regions.

After the edges of the defective regions of the CT are determined using edge detection methods, a morphological operator is used to fill in the detected regions [3, 4, 13]. In all the morphological processes, structuring elements are used. There are different structuring elements such as diamond, disk, and octagon [18]. Each structuring element has its own parameter. A proper structuring element and parameter selection is important.

The structuring elements and parameters used in this paper are shown in Table 1.

Table 1 The structuring elements and parameters used in this paper

Structuring Element	Parameter
diamond	R
disk	R
octagon	R
line	LEN, DEG
square	W

The parameter R shown in Table 1, specifies the distance for the diamond and octagon, and the radius for the disk. For the line, the parameters LEN and DEG specify length and angle, respectively. The parameter W specifies the width for the square. We used the closing morphology operator. The morphological closing of I by S, denoted I • S, is defined by Eq. (3) [18].

$$I \bullet S = (I \oplus S) \ominus S \tag{3}$$

where I is a binary image, and S is a matrix of 0s and 1s that specifies the structuring element. The closing morphology operator is a dilation followed by an erosion as shown in Eq. (3). While the dilation operator fills the intra borders of defective regions, erosion operator eliminates the extra borders of defective regions.

2.3. Derivation of the Proposed Method

This paper provided the derivation of a new gradient-based surface defect detection (GBSDD) method for CT images. In this method, one or more homogeneous regions in the image are selected first. According to the selected regions, a threshold value and mean pixel value are calculated. Then, a reference pixel is determined in the CT image. By comparing the reference pixel with the relevant pixel in the CT image, it is determined whether the relevant pixel is defective. The GBSDD method has two steps: 1- Determination of threshold and mean pixel values. 2- Obtaining the defective pixels in the CT image using these values.

2.3.1. Determination of Threshold and Mean Pixel Values

To calculate the threshold value (T) and the mean pixel value (P_{mean}), first, a homogeneous region is selected in the CT image as shown in Fig. 5.

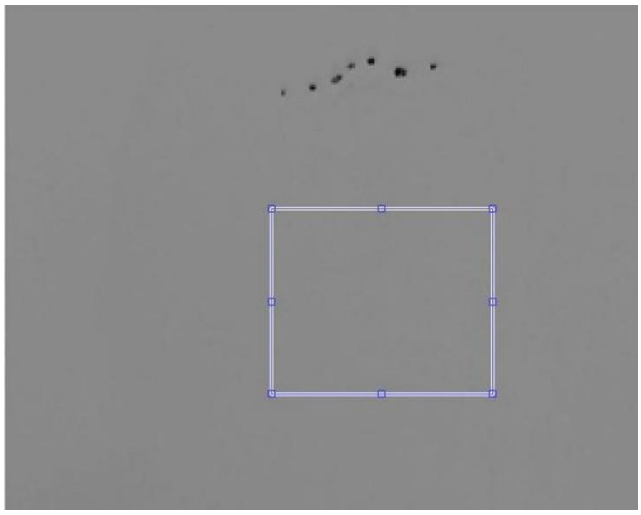

Figure 5 Selected homogenous region in the gray level image

The row and column numbers of the selected part of the image are m_s and n_s, respectively. Then, Eq. (4) is computed for each pixel in the first row of the selected region

$$T_x = |I(x) - I(x+1)|$$

$$for\ x = 1, 2, 3, \ \ldots, n_s - 1 \tag{4}$$

where "I(x) - I(x+1)" indicates the difference between the two horizontally adjacent pixels. After calculating the threshold values for the first row, (n_s-1) number of threshold values are obtained. For each row in the selected region, Eq. (4) is repeated. Finally, the maximum value (T_{xmax}) is selected among ((n_s-1) * m_s) number of threshold values for the horizontal direction.

Then, Eq. (5) is computed separately for each column in the selected region

$$T_y = |I(y) - I(y+1)|$$

$$for\ y = 1, 2, 3, \ldots, m_s - 1 \tag{5}$$

where "I(y) - I(y+1)" indicates the difference between the two vertically adjacent pixels. After calculating all the threshold values, the maximum value (T_{ymax}) is selected among ((m_s-1) * n_s) number of threshold values for the vertical direction.

If the number of selected homogeneous regions (h) is z, then z number of T_{xmax} (T_{xmax1}, T_{xmax2}, T_{xmax3}, …T_{xmaxz}) and z number of T_{ymax} (T_{ymax1}, T_{ymax2}, T_{ymax3}, …T_{ymaxz}) values are obtained. After eliminating max {T_{xmax1}, T_{xmax2}, T_{xmax3}, …T_{xmaxz}} and max {T_{ymax1}, T_{ymax2}, T_{ymax3}, …T_{ymaxz}}, the mean value of the remaining values is calculated (T_m).

Finally, T is calculated by Eq. (6)

$$T = T_m + dp \tag{6}$$

where dp is the defect parameter. dp determines the sensitivity of the defective detected. Larger values of dp decrease the sensitivity.

The second parameter, P_{mean}, is obtained by calculating the mean value of the pixels in the selected region. If more than one region is selected, the mean of the obtained P_{mean} values is calculated. As the number of selected homogeneous regions increases, the accuracy of the proposed method increases, but the processing time also increases.

2.3.2. Obtaining Defective Pixels in the CT Image

The detailed block diagram of the proposed defect detection algorithm is shown in Fig. 6. First, the proposed algorithm shown in Fig. 6 is applied for the first row. The first pixel in the row is determined as the reference pixel (I(r)). The reference pixel is compared with the pixel just to the right. The aim is to determine whether the compared pixel (I(c)) is defective. If the following two conditions are met, I (c) is determined as defective.

$$|I(r) - I(c)| > T$$

and

$$I(c) > (P_{mean} + T) \; or \; I(c) < (P_{mean} - T)$$

If I(c) is defective, the pixel just to the right of the I(c) becomes the new pixel to be compared (I(c) = I(c+1)). Then I(r) is compared with the I(c) to determine whether the I(c) is defective. When I(c) is not defective, the compared pixel becomes the new reference pixel. Then the obtained reference pixel is compared with the pixel just to the right. This process continues until the last pixel in the corresponding row is involved in the process. For each row in the CT image, the above algorithm is repeated. As a result, a defective binary image is obtained according to the detected defective and non-defective pixels. The pixel in the obtained image is "1" if it is defective, otherwise, it is "0".

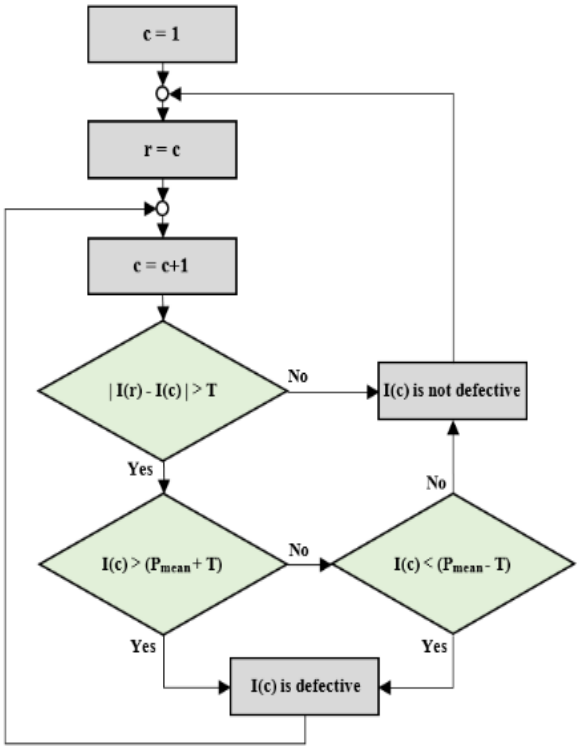

Figure 6 Block diagram of the proposed defect detection algorithm

Let's show a CT image by using pixels as in Fig. 7.

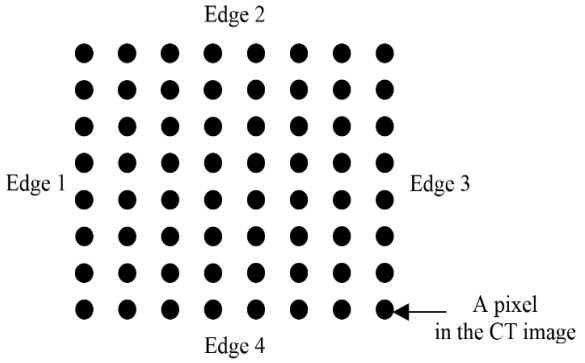

Figure 7 CT image represented by pixels

A CT has four edges, and each edge was numbered as shown in Fig. 7: Edge 1, Edge 2, Edge 3 and Edge 4. The defect detection algorithm mentioned above is repeated four times, with each edge selected as the starting edge. The starting edge is Edge 1 for Fig. 7. Fig. 8 shows when the starting edges are Edge 2, Edge 3 and Edge 4.

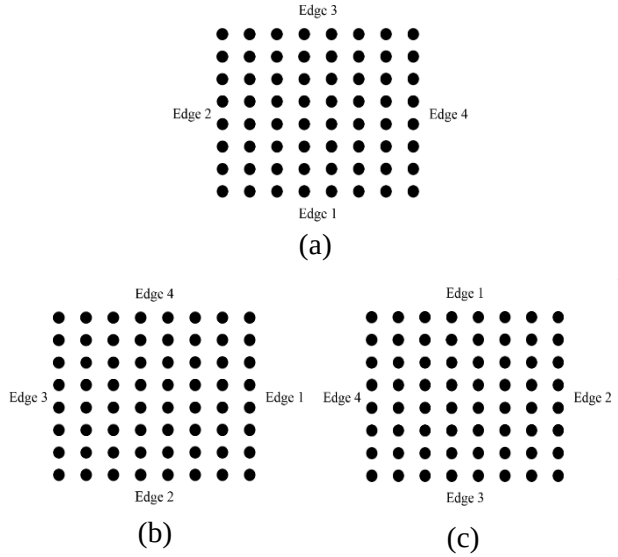

Figure 8 The starting edge is (a) Edge 2 (b) Edge 3 (c) Edge 4

Thus, four defective binary images are obtained for the four starting edges. For the final defective binary image, the obtained four defective binary images are combined according to Eq. (7).

$$I(i,j) = \left(I_{e1}(i,j) | I_{e3}(i,j)\right) \,\&\, \left(I_{e2}(i,j) | I_{e4}(i,j)\right)$$
$$for\ i = 1,2,3,\dots,N\ and\ j = 1,2,3,\dots,M \quad (7)$$

where $I_{e1}(i,j)$, $I_{e2}(i,j)$, $I_{e3}(i,j)$ and $I_{e4}(i,j)$ are the pixels at position (i,j) in the defective binary images when the starting edges are Edge 1, Edge 2, Edge 3 and Edge 4, respectively. I(i,j) is the pixel at position (i,j) in the final defective binary image, M and N are the sizes of the CT image. According to Eq. (7), if at least one of the $I_{e1}(i,j)$ and $I_{e3}(i,j)$ values and at least one of the $I_{e2}(i,j)$ and $I_{e4}(i,j)$ values are "1", the value of I(i,j) in the defective binary image is "1", otherwise its value is "0".

A CT image and its defective binary image are shown in Fig. 9.

(a) (b)

Figure 9 (a) Original CT image (b) defective binary image

The defective binary image shown in Fig. 9b was obtained from the original image shown in Fig. 9a using the GBSDD method. The non-defective and defective pixels are shown as black and white in Fig. 9b, respectively.

The proposed method cannot be applied to tiles with defects on the edges. It is accepted that there is no defective pixel on the edge of the CT image. Besides that, if the image has regions containing edge, these regions can be identified as a defect after the proposed method. These regions are image specific and known, so these edge regions are eliminated before the defect detection method is applied.

3. RESULTS AND DISCUSSION

To evaluate the GBSDD method, we used the existing gradient-based methods: Sobel, Prewitt and Canny, both with and without the morphological operator, six CT images which

were RI1, RI2, RI3, SI1, SI2, SI3 for objective evaluation and four CT images for subjective evaluation. We applied the structuring elements and the different values of the parameters, shown in Table 1, when the morphological operator was used. Table 2 gives the obtained best results using the existing methods for RI1, RI2 and RI3.

Table 2 The best results obtained with the existing method for RI1, RI2 and RI3

Images	DAR and its parameters	The type of method with the best result
RI1	99.9547	Prewitt+Square (W=3)
	A=72, B=4, C=22, D=57254	
RI2	99.4997	Prewitt
	A=21, B=448, C=50, D=99027	
RI3	99.577	Prewitt+Line (LEN=14, DEG=45)
	A=312, B=337, C=100, D=102571	

Among the existing gradient-based methods for RIs, Table 2 shows that the best performance was Prewitt. While the best results were obtained by using the morphological operator for RI1 and RI3, the best results were obtained for RI2 without the morphological operator. The defective binary images corresponding to the best results for all three images are shown in Fig. 10.

For RIs, the obtained results and defective binary images using the proposed method are given in Table 3 and Fig. 11, respectively.

For the proposed method, eight homogeneous regions were selected. Then T and P_{mean} were calculated by selecting different dp values for the three images. When the results obtained after applying the proposed method are compared with the results shown in Table 2, the proposed method gives better results than the existing methods for all three images. Comparing Fig. 10 with Fig. 11, the proposed method better identifies both defective and non-defective regions.

For SIs, the obtained results and images for both the existing and the proposed methods are given in Tables 4-5 and Figs. 12-13.

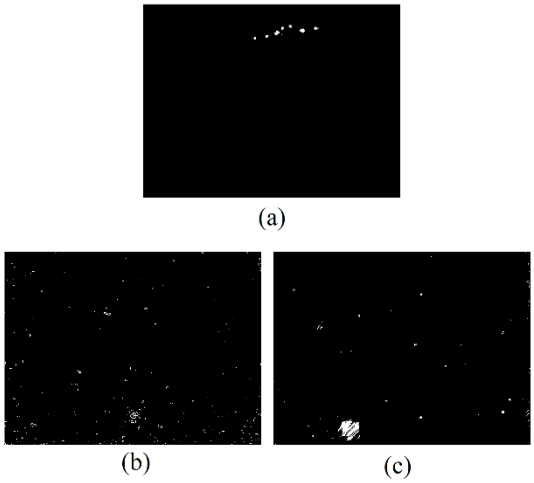

Figure 10 Obtained defective binary images using existing methods corresponding to the best results for (a) RI1 (b) RI2 (c) RI3

Table 3 The obtained results with the GBSDD method for RI1, RI2 and RI3

Images	DAR and its parameters	The proposed method parameters
RI1	99.9983	dp=4, h=8
	A=93, B=0, C=1, D=57258	
RI2	99.9879	dp=1, h=8
	A=61, B=2, C=10, D=99473	
RI3	99.9642	dp=1, h=8
	A=385, B=10, C=27, D=102898	

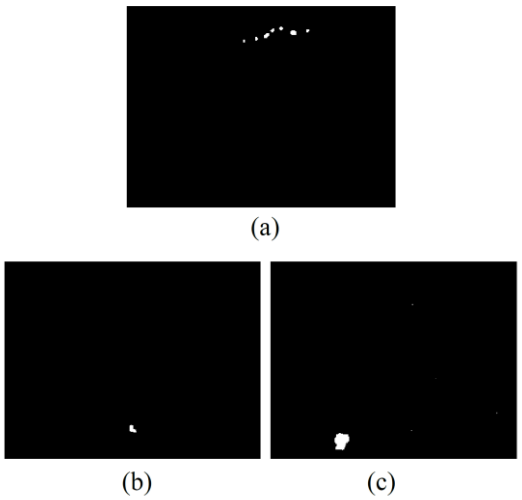

Figure 11 The obtained defective binary images using the GBSDD method for (a) RI1 (b) RI2 (c) RI3

Table 4 The best results obtained with the existing method for SI1, SI2 and SI3

Images	DAR and its parameters	The type of method with the best result
SI1	99.8949	Sobel+Disk (R=4)
	A=152, B=103, C=0, D=97745	
SI2	99.8776	Sobel+Disk (R=3)
	A=60, B=120, C=0, D=97820	
SI3	99.9255	Sobel+Diamond (R=4)
	A=89, B=73, C=0, D=97838	

(a)

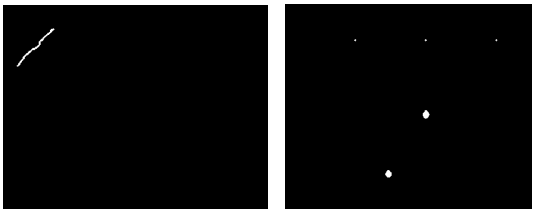

(b) (c)

Figure 12 Obtained defective binary images using existing methods corresponding to the best results for (a) SI1 (b) SI2 (c) SI3

Table 5 The obtained results with the GBSDD method for SI1, SI2 and SI3

Images	DAR and its parameters	The proposed method parameters
SI1	100	dp=0, h=8
	A=152, B=0, C=0, D=97848	
SI2	100	dp=0, h=8
	A=60, B=0, C=0, D=97940	
SI3	100	dp=0, h=8
	A=89, B=0, C=0, D=97911	

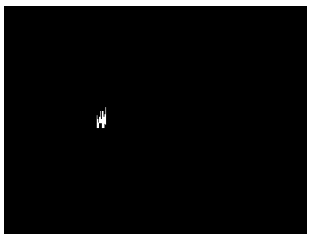

(a)

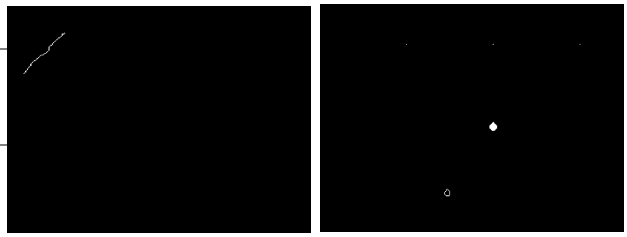

(b) (c)

Figure 13 The obtained defective binary images using the GBSDD method for (a) SI1 (b) SI2 (c) SI3

As in the RIs, eight homogeneous regions were selected within the SIs. Table 4 shows that the best performance was Sobel among the existing gradient-based methods for SIs. As shown in Table 4, parameter B negatively affected the results. Table 5 shows the proposed method gives excellent results for SIs. There is no wrongly identified pixel for the output images of the proposed method. If we compare Fig. 4 with Figs. 12 and 13, it is understood that the GBSDD method has a better performance than the existing methods.

Table 5 shows the values of the dp were determined as zero for all SIs. For the RIs, different dp values were determined as shown in Table 3. If the values of dp in Eq. (6) are selected as zero for all RIs, the obtained DAR values were 99.9686, 99.9859 and 99.9555 for RI1, RI2 and RI3, respectively. If we compare these DAR values with DAR values in Table 2, the values obtained for dp = 0 are bigger than the best results obtained with the existing method. For improving the defective binary image, the value of the dp parameter is important. The DAR values shown in Table 3 are bigger than the DAR values obtained for dp = 0. For example, Fig. 14 shows the reference and the defective binary images obtained using the GBSDD method for RI3 when dp=0 and dp=1.

(a)

(b)

(c)

Figure 14 The reference and defective binary images obtained using the GBSDD method for the RI3 (a) reference image (b) dp = 0 (c) dp = 1

When Fig. 14a is examined, there are very small defective pixels. Comparing Fig. 14b with Fig. 3c, invisible defects by people can be determined by the proposed method. Moreover, a better defective binary image can be obtained as shown in Fig. 14c by increasing the dp value. Increasing the dp value too much can cause these pixels to disappear.

Finally, the tests were carried out with some real CT images, shown in Fig. 15, for subjective evaluation. There is no reference image for these images. The obtained defective binary images using the GBSDD method are shown in Fig. 16. By comparing Fig. 15 and Fig. 16, it can be seen that the GBSDD method has good defect detection capability.

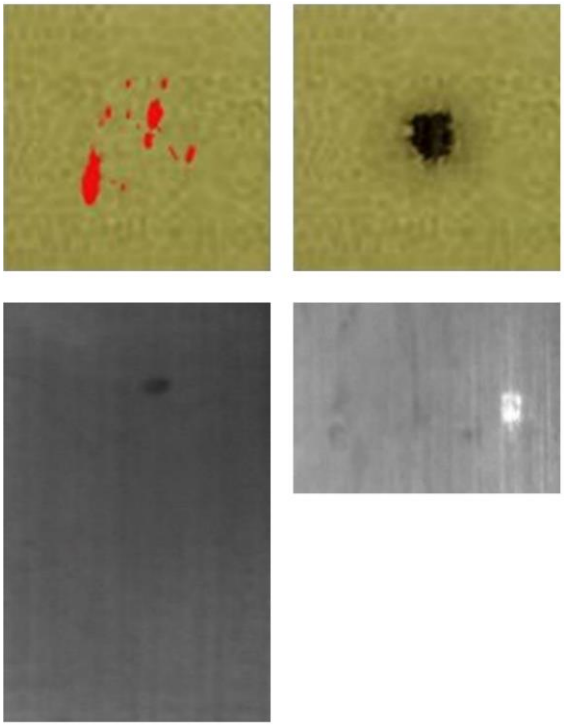

Figure 15 Real CT images for subjective evaluation

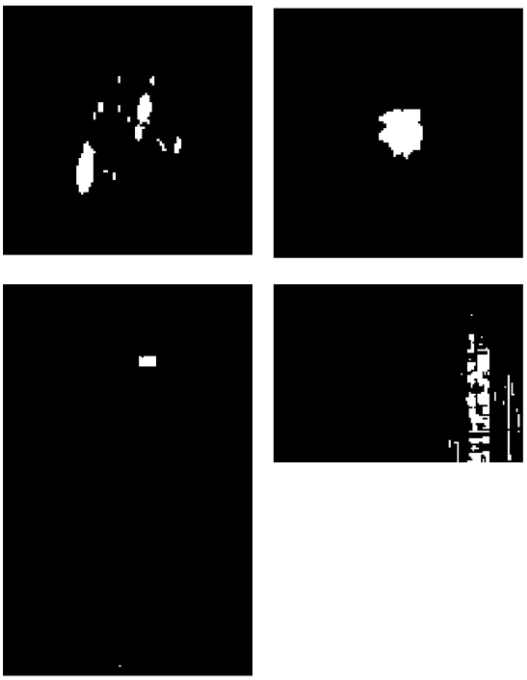

Figure 16 Defective binary images of the CT images shown in Fig. 15

Image processing methods have been used in the ceramic industry for various purposes [19]. Our target is to detect the surface defects for the CT using the image processing method we developed. The tests carried out on the CT images show that the proposed method assures a good performance.

4. CONCLUSIONS

In this paper, we proposed a new method, GBSDD, as a way to detect the surface defects of CTs. For this purpose, one or more homogeneous regions in the CT image are selected. After calculating the threshold and mean pixel values, the reference pixel is compared to another pixel in the image to determine whether the compared pixel is defective. If the compared pixel is defective, the same reference pixel is compared with another pixel. When the compared pixel is not defective, the reference pixel changes. Thus, the defective binary image showing defective and non-defective regions of the CT image is obtained. The obtained results show us that the proposed method assures a good performance, and as such, we recommend it as a useful method.

Acknowledgments
The author thanks S. H. Hanzaei, A. Afshar and F. Barazandeh for providing the real CT images.

Funding
The author has no received any financial support for the research, authorship or publication of this study.

The Declaration of Conflict of Interest/ Common Interest
No conflict of interest or common interest has been declared by the authors.

The Declaration of Ethics Committee Approval
This study does not require ethics committee permission or any special permission.

The Declaration of Research and Publication Ethics
The authors of the paper declare that they comply with the scientific, ethical and quotation rules of SAUJS in all processes of the paper and that they do not make any falsification on the data collected. In addition, they declare that Sakarya University Journal of Science and its editorial board have no responsibility for any ethical violations that may be encountered, and that this study has not been evaluated in any academic publication environment other than Sakarya University Journal of Science.

REFERENCES

[1] M. H. Karimi, D. Asemani, “Surface defect detection in tiling Industries using digital image processing methods: Analysis and evaluation”, ISA transactions, vol. 53, no. 3, pp. 834-844, 2014.

[2] T. Czimmermann, G. Ciuti, M. Milazzo, M. Chiurazzi, S. Roccella, C. M. Oddo, P. Dario, “Visual-Based Defect Detection and Classification Approaches for Industrial Applications—A SURVEY”, Sensors, vol. 20, no. 5, pp. 1459, 2020.

[3] G. M. Rahaman, M. Hossain, “Automatic defect detection and classification technique from image: a special case using ceramic tiles”, International Journal of Computer Science and Information Security, vol. 1, no. 1, pp. 22-30, 2009.

[4] S. H. Hanzaei, A. Afshar, F. Barazandeh, “Automatic detection and classification of the ceramic tiles’ surface defects”, Pattern Recognition, vol. 66, pp. 174-189, 2017.

[5] A. Mohan, S. Poobal, “Crack detection using image processing: A critical review and analysis”, Alexandria Engineering Journal, vol. 57, no. 2, pp. 787-798, 2018.

[6] A. N. Shire, M. M. Khanapurkar, R. S. Mundewadikar, "Plain ceramic tiles surface defect detection using image processing", in 2011 Fourth International Conference on Emerging Trends in Engineering & Technology, pp. 215-220, November 2011.

[7] H. F. Ng, "Automatic thresholding for defect detection", Pattern recognition letters, vol. 27, no. 14, pp. 1644-1649, 2006.

[8] Z. Hocenski, T. Keser, A. Baumgartner, "A simple and efficient method for ceramic tile surface defects detection", in 2007 IEEE International Symposium on Industrial Electronics, pp. 1606-1611, June 2007.

[9] A. Sioma, "Automated Control of Surface Defects on Ceramic Tiles Using 3D Image Analysis", Materials, vol. 13, no.5, pp. 1250, 2020.

[10] A. Latif-Amet, A. Ertüzün, A. Erçil, "An efficient method for texture defect detection: sub-band domain co-occurrence matrices", Image and Vision computing, vol. 18, no. 6-7, pp. 543-553, 2000.

[11] S. Vasilic, Z. Hocenski, "The edge detecting methods in ceramic tiles defects detection", in 2006 IEEE International Symposium on Industrial Electronics, pp. 469-472, July 2006.

[12] Z. Hocenski, T. Keser, "Failure detection and isolation in ceramic tile edges based on contour descriptor analysis", in 2007 Mediterranean Conference on Control & Automation, pp. 1-6, June 2007.

[13] Y. C. Samarawickrama, C. D. Wickramasinghe, "Matlab based automated surface defect detection system for ceremic tiles using image processing", in 2017 6th National Conference on Technology and Management (NCTM), pp. 34-39, January 2017.

[14] Matlab, Image Processing Toolbox.

[15] I. Sobel, "Camera models and perception", Ph.D. thesis, Stanford University, CA, 1970.

[16] J. Prewitt, "Object Enhancement and Extraction. Picture Processing and Psychopictorics", NY, Academic Pres., 1970.

[17] J. Canny, "A Computational approach to edge detection", IEEE Transactions on Pattern Analysis and Machine Intelligence, vol. 8, pp. 679-700, 1986.

[18] R. C. Gonzalez, R. E. Woods, S. L. Eddins, "Digital Image Processing Using MATLAB", Saddle River, NJ, Pearson Prentice Hall., 2004.

[19] S. Chowdhury, D. Dhara, S. Chowdhury, P. Haldar, K. Chatterjee, T. K. Bhattacharya, "A novel approach toward microstructure evaluation of sintered ceramic materials through image processing techniques", International Journal of Applied Ceramic Technology, vol. 18, no. 3, pp. 773-780, 2021.